JCTC Journal of Chemical Theory and Computation

Article

pubs.acs.org/JCTC

Characterization of the *t*-Butyl Radical and Its Elusive Anion

Alexander Yu. Sokolov,* Samyak Mittal, Andrew C. Simmonett, and Henry F. Schaefer, III

Center for Computational Quantum Chemistry, The University of Georgia, Athens, Georgia 30602, United States

Supporting Information

ABSTRACT: The *t*-butyl radical and its anion are studied theoretically using state-of-the-art quantum mechanical methods including coupled cluster theory with full single, double, and triple excitations (CCSDT) and CCSDT with perturbative quadruple excitations [CCSDT(Q)], in concert with large correlation-consistent cc-pVXZ and aug-cc-pVXZ (X = D, T, Q, 5) basis sets. The relative energies are extrapolated to the complete basis set limit (CBS). The lowest energy structure of the *t*-butyl radical has a nonplanar carbon backbone with overall C_{3v} symmetry. Low-lying C_{3h} and C_s symmetry transition states, for pyramidal inversion and methyl group rotation, respectively, between equivalent C_{3v} minima are investigated. The barriers for these interconversions are both less than 1 kcal mol^{-1}, but the corresponding barriers on the anion potential energy surface are more pronounced. Using the focal point analysis technique, we obtain a value of −0.48 kcal mol^{-1} for the *t*-butyl radical adiabatic electron affinity at the CCSDT(Q)/CBS level of theory, where the negative sign indicates that the formation of the *t*-butyl anion is adiabatically unfavorable. We show that the electron affinity, whose sign has been the subject of debate, is very sensitive to both the basis set and the correlation treatment, and previous experimental and theoretical estimates of its value bracket the value computed herein. Our results indicate that the *t*-butyl anion is classically metastable with a vertical detachment energy of over 10 kcal mol^{-1} to reach the neutral potential energy surface. However, the inclusion of the zero-point vibrational effects seems to favor its nonexistence.

INTRODUCTION

The reactivity of alkyl radicals is conducive to rich and varied chemistry. Consequently, they play an important role in many chemical subdisciplines, including organic, polymer, combustion, planetary atmospheric, and interstellar chemistry.[1,2] For example, they occur as intermediate species in the industrial thermal cracking of hydrocarbons for the production of olefins.[3−5] Alkyl radicals also play a vital role in determining reaction pathways and pollutant formation.[6−8] However, the high reactivity of these radicals, coupled with low barriers to isomerization, complicates their isolation and characterization, and they are generally not as well understood as their closed-shell alkane progenitors.[9]

As the simplest tertiary alkyl radical, the *t*-butyl radical serves as an important model system for a large class of radicals and has therefore received considerable attention in previous experimental and theoretical studies. In 1972, Wood and co-workers[10] performed electron paramagnetic resonance studies of the *t*-butyl radical. Their experimental results suggested that the structure of the radical is nonplanar. Further evidence for a pyramidal structure was obtained in a 1975 photoelectron spectroscopy study.[11] In 1976, Krusic and Meakin carried out another electron spin resonance experiment, from which the barrier for pyramidal inversion was estimated to be 0.64 kcal mol^{-1}.[12]

In 1981, Pacansky and Yoshimine[13] reported the first theoretical study of the *t*-butyl radical ground state structure using the unrestricted Hartree−Fock (UHF) method. In their work, the equilibrium structure of the radical was found to have C_{3v} symmetry; this result was later confirmed by a matrix isolation study,[14] which provided the first infrared vibrational spectrum of the *t*-butyl radical. At the same time, Paddon-Row and Houk,[15] also using the UHF method, concluded that the radical has a pyramidal C_{3v} structure. They proposed that the pyramidal inversion of the structure proceeds through a planar C_{3h} symmetry transition state and computed the barrier to inversion to be 1.2 kcal mol^{-1}. The stabilization of the pyramidal structure was attributed to the hyperconjugative effect and lower torsional interactions between the methyl groups and the radical center. In 1991, Pacansky and co-workers reported the first theoretical harmonic vibrational frequencies of the radical, also using the UHF method.[16] Very recently, the structures, harmonic frequencies, barrier to inversion, and ionization potential of the *t*-butyl radical were studied using several density functional theory (DFT) methods.[17] Strong dependence of the results on the choice of the method was noted. The barrier to pyramidal inversion was computed to be in the range of 0.9−1.2 kcal mol^{-1}.

The electron affinity of the *t*-butyl radical has been the subject of controversy. In 1986, Schleyer and Spitznagel[18] predicted the electron affinity to be −9.6 kcal mol^{-1}, which indicated the thermodynamic instability of the carbanion. In 1989, Depuy and co-workers[19] using the flow tube experiment determined the gas-phase acidity of isobutane, from which the *t*-butyl radical electron affinity was derived to be −5.9 kcal mol^{-1}. Another negative value of the electron affinity (−3.5 kcal mol^{-1}) was computed by Vera and Pierini[20] using DFT with the B3LYP functional. In a 1999 computational study, Sauers[21] reported electron affinities of the *t*-butyl radical ranging from −1.05 kcal mol^{-1} at the B3LYP level of theory to +3.02 kcal mol^{-1} at the second-order Møller−Plesset perturbation theory level (MP2), thus indicating that some of the theoretical methods predict the formation of the *t*-butyl anion to be

Received: August 30, 2012
Published: September 25, 2012

   dx.doi.org/10.1021/ct300753d | J. Chem. Theory Comput. 2012, 8, 4323−4329

favorable. Furthermore, a recent (2008) theoretical study[22] using the composite G3MP2B3 method reported the *t*-butyl radical electron affinity to be +3.2 kcal mol^{-1}.

Despite the aforementioned work, a precise structure for *t*-butyl has not been proposed. Given the availability of accurate theories to investigate chemical systems of this size, we will characterize the *t*-butyl radical, paying close attention to the structures and relative energies of the different conformers. Furthermore, we aim to resolve the controversy surrounding its gas-phase electron affinity, by investigating the anion. Our findings for the neutral and anionic systems will be compared to those for the *t*-butyl cation,[23] which originally spurred our interest in this system.

METHODS

To accurately characterize both the *t*-butyl radical and anion, we employed coupled cluster methods incorporating single and double excitations (CCSD)[24−27] and CCSD with perturbative triple excitations [CCSD(T)].[27−29] Unrestricted coupled cluster methods, with restricted open-shell Hartree−Fock (ROHF) references, were used for the neutral, open-shell species. Equilibrium structures and harmonic vibrational frequencies for the *t*-butyl radical and anion were obtained at the all-electron CCSD(T) level with Dunning's correlation-consistent polarized-core-valence cc-pCVTZ basis set.[30,31] Tight convergence criteria were used for the energy (10^{-10} E_h) and the root-mean-square of the energy gradient (10^{-6} E_h/a_0). For all stationary points, the wave functions were found to have a dominant contribution from a single Slater determinant.

The electron affinity of the *t*-butyl radical, as well as the energy barriers for pyramidal inversion and methyl rotation of the radical and the anion, were obtained via the focal point analysis technique[32,33] using the CCSD(T)/cc-pCVTZ optimized geometry. Complete basis set (CBS) limit values were obtained by extrapolating the Hartree−Fock (E_{HF}) and the correlation energies (E_{Corr}) employing the cc-pVXZ and aug-cc-pVXZ (X = D, T, Q, 5) families of basis sets,[30] using the functional forms[34,35]

$$E_{HF}(X) = E_{HF}^{\infty} + ae^{-bX} \quad (1)$$

and

$$E_{Corr}(X) = E_{Corr}^{\infty} + aX^{-3} \quad (2)$$

respectively. Higher-order correlation effects were accounted for using coupled cluster theory including all single-, double-, and triple excitations (CCSDT) and also the perturbative quadruple corrections [CCSDT(Q)] thereto.[36] In the focal point extrapolations, only valence electrons were correlated. The final values were obtained by adding auxiliary core correlation Δ_{core} and zero-point vibrational energy Δ_{ZPVE} corrections. The core correlation correction Δ_{core} was determined by the difference between all-electron and frozen-core CCSD(T)/cc-pCVTZ results. The Δ_{ZPVE} correction was computed using harmonic vibrational frequencies obtained at the all-electron CCSD(T)/cc-pCVTZ level of theory. Augmenting the cc-pCVTZ basis set with diffuse functions makes the CCSD(T) method prohibitively expensive for geometry optimization and vibrational analyses of the *t*-butyl and its anion. However, when comparing an anion and a neutral, there is less scope for error cancellation, and the diffuse functions are expected to more significantly affect the anion due to the diffuse character of the extra electron; to obtain an estimate of this effect, the difference between zero point corrections from MP2/aug-cc-pVTZ and MP2/cc-pVTZ vibrational frequencies, $\Delta_{aug-ZPVE}$, was appended to our final result. Finally, relativistic effects (Δ_{rel}) were accounted for by adding the mass-velocity and Darwin one-electron terms computed at CCSD(T)/cc-pCVTZ level of theory.

All computations were performed with the CFOUR[37] and MOLPRO software packages,[38] with the exception of CCSDT and CCSDT(Q), which came from the MRCC program of Kállay[39,40] as interfaced to MOLPRO.

RESULTS AND DISCUSSION

Structures and Relative Energies. The lowest-energy structure of the *t*-butyl radical optimized at the CCSD(T)/cc-pCVTZ level of theory is presented in Figure 1. The structure

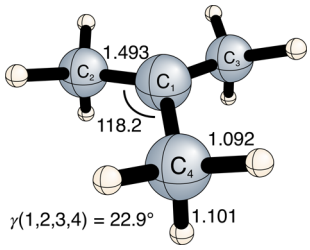

Figure 1. Structure of the ground state of the *t*-butyl radical (C_{3v} symmetry) optimized at the CCSD(T)/cc-pCVTZ level of theory. Bond lengths are in Ångstroms; angles are in degrees. Parameter $\gamma(1,2,3,4)$ denotes the angle of the C_1-C_2 bond out of the $C_1-C_3-C_4$ plane. Only unique structural parameters are shown.

has C_{3v} symmetry and is slightly nonplanar, possessing an out-of-plane angle between the carbon of the methyl group and the plane formed by the remaining three carbon atoms [$\gamma(1,2,3,4)$, *c.f.* Figure 1] of 22.9°; this is significantly smaller than that of a perfect tetrahedron (54.7°). The methyl groups are oriented such that the axial C−H bonds are parallel and antiperiplanar to the singly occupied p orbital on the central carbon. This *trans* arrangement affords negative hyperconjugation of the unpaired electron into the axial C−H antibonding orbitals,[41−44] as evidenced by the *ca* 0.01 Å elongation of the axial C−H bonds relative to the equatorial C−H bonds. Natural bond orbital (NBO)[45,46] analyses reveal a decrease in the occupation of the NBO describing the unpaired electron and a corresponding increase in the population of the antibonding σ^*(C−H) NBO, which is further evidence for negative hyperconjugation. In contrast to the radical, the global minimum structure for the *t*-butyl cation has C_s symmetry and a nearly planar carbon backbone [$\gamma(1,2,3,4) = 0.6°$];[23] the vacant p orbital is stabilized by conventional hyperconjugation interactions, which require a more nearly planar geometry to maximize overlap with the C−H σ orbitals.

Figures 2 and 3 show the C_{3h} and C_s symmetry stationary points on the *t*-butyl radical ground electronic state potential energy surface, respectively. The C_{3h} structure represents a transition state for the pyramidal inversion of the global minimum C_{3v} structure along the C_3 symmetry axis, while the C_s structure is a transition state for the rotation of a methyl group (Figure 4). Focal point analysis reveals that the C_{3h} structure lies 0.74 kcal mol^{-1} above the global minimum at the CCSD(T)/CBS level of theory (Table 1 and Figure 4). This value is in very good agreement with estimations of the pyramidal inversion barrier from electron spin resonance

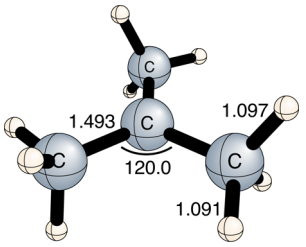

Figure 2. Structure of the C_{3h} transition state of the *t*-butyl radical optimized at the CCSD(T)/cc-pCVTZ level of theory. Bond lengths are in Ångstroms; angles are in degrees. Only unique structural parameters are shown.

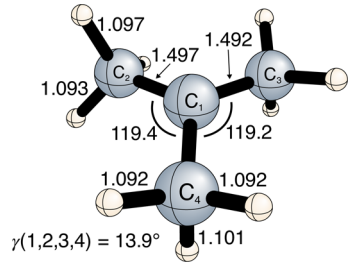

Figure 3. Structure of the C_s transition state of the *t*-butyl radical optimized at the CCSD(T)/cc-pCVTZ level of theory. Bond lengths are in Ångstroms; angles are in degrees. The parameter $\gamma(1,2,3,4)$ denotes the angle of the C_1-C_2 bond out of the $C_1-C_3-C_4$ plane. Only unique structural parameters are shown.

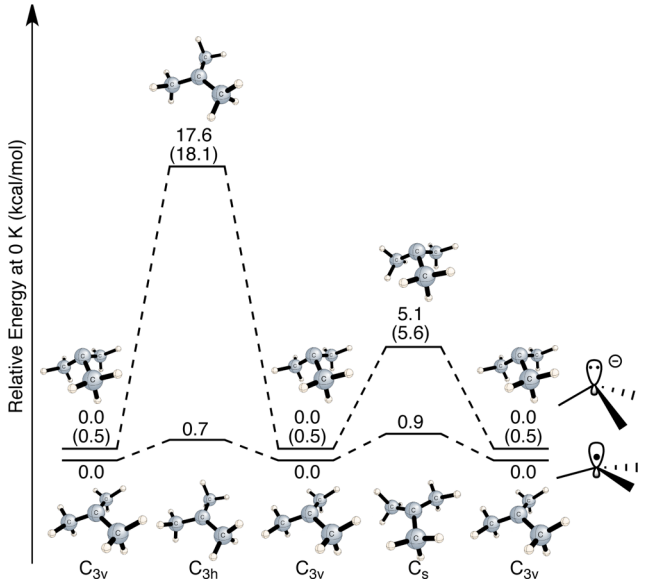

Figure 4. Schematic potential energy surfaces of the *t*-butyl radical and anion. The energies of the C_s and C_{3h} structures are relative to the C_{3v} global minimum structure on the same potential surface. Values in parentheses are relative energies of the *t*-butyl anion structures with respect to the energy of the C_{3v} symmetry *t*-butyl radical. Relative energies (in kcal mol^{-1}) were computed at the CCSD(T)/CBS level of theory (see Tables 1 and S1–S3). The relative energy of the C_{3v} structure of the *t*-butyl anion was computed at the CCSDT(Q)/CBS level (Table 2).

experiments (0.64 kcal mol^{-1}).[12] The C_s structure is 0.85 kcal mol^{-1} above the global minimum structure (Table S1 and Figure 4), which indicates a low-energy barrier for methyl rotation. Distortion of the C_{3v} structure to C_{3h} and C_s does not significantly affect the C–C and C–H bond distances. In the C_s structure, a 0.005 Å lengthening of the symmetry–distinct C–C bond is observed as a result of the rotation of the methyl group. This structural effect is accompanied by a reduction in the out-of-plane $\gamma(1,2,3,4)$ angle from 22.9° in the C_{3v} structure to 13.9° in the C_s structure. In both transition states, the C–H bonds are more nearly equalized, indicating that the effect of hyperconjugation for these structures is smaller than for C_{3v}.

The C_{3v}, C_{3h}, and C_s structures of the *t*-butyl anion are shown in Figures 5, 6, and 7, respectively. Like the neutral, the global minimum structure has C_{3v} symmetry. The C_{3h} and C_s structures are transition states of the same nature as for the *t*-butyl radical (*c.f.* Figures 2 and 3). The C_{3v} and C_s structures of the anion are significantly more pyramidalized than their radical analogs with out-of-plane angles for the carbon framework, $\gamma(1,2,3,4)$, of 60.6° and 58.2°, respectively. This structural difference can be rationalized by simple VSEPR arguments and is due to the extra repulsive interactions from the lone pair localized on the central carbon atom and the C–C bonds of the methyl groups. All C–C distances of the C_{3v} and C_s *t*-butyl anion structures are increased by ~0.02–0.04 Å as a result of the presence of excess electric charge. Interestingly, the C–C bond lengths of the C_{3h} anion structure are actually shorter in comparison to the values for the radical; this is a manifestation of negative hyperconjugation of the lone pair into the axial σ^*(C–H) orbitals. There is a concomitant increase in the axial C–H bond lengths, which are over 0.03 Å longer than their equatorial counterparts. The equatorial C–H distances are only affected by ~0.005 Å. Energetically, the C_s transition state is 5.05 kcal mol^{-1} above the C_{3v} global minimum (Table S2), yielding a much larger barrier for the methyl rotation of the *t*-butyl anion than that for the radical (Figure 4). The planar C_{3h} structure of the anion is highly unfavorable, lying 17.68 kcal mol^{-1} relative the global minimum (Table S3). This result once again illustrates the preference of the *t*-butyl anion for the strongly puckered structure, which gives rise to the high barrier for pyramidal inversion.

Harmonic Vibrational Frequencies. Harmonic vibrational frequencies for the C_{3v} global minimum structure of the *t*-butyl radical and anion computed at CCSD(T)/cc-pCVTZ level of theory are presented in Tables S4 and S5, respectively. The most notable feature of the vibrational spectrum of the C_{3v} *t*-butyl radical is the presence of two well-separated groups of vibrational modes in the C–H stretching region at 2953–2960 and 3058–3110 cm^{-1}. The lower-frequency modes correspond to stretching vibrations of the axial C–H bonds, while the modes of higher frequency are dominated by the stretches of equatorial C–H bonds. The separation of the axial and equatorial C–H stretching modes in vibrational energy is further evidence of the aforementioned hyperconjugation effects. The vibrational modes responsible for the C–C bond stretching motion are located at 770 and 1016 cm^{-1} within the harmonic approximation. Our theoretical harmonic frequencies are in general agreement with the fundamental frequencies obtained from an infrared matrix isolation experiment.[13] The vibrational spectrum of the C_{3h} *t*-butyl radical structure exhibits one imaginary frequency of 180*i* cm^{-1} corresponding to the out-of-plane motion of carbon atoms characteristic of pyramidal inversion. The C_s structure also has one imaginary frequency (139*i* cm^{-1}) corresponding to the internal rotation of the methyl group around the C–C bond.

Table 1. Focal Point Analysis of the C_{3h} Transition State Energy of the *t*-butyl Radical Relative to the C_{3v} Global Minimum Structure (ΔE_v, kcal mol^{-1})[a]

basis set	ΔE_e[ROHF]	δ[MP2]	δ[CCSD]	δ[CCSD(T)]	ΔE_e[CCSD(T)]
cc-pVDZ	+1.98	−0.44	−0.06	+0.04	[+1.52]
cc-pVTZ	+2.18	−0.76	+0.02	+0.01	[+1.44]
cc-pVQZ	+2.23	−0.79	+0.04	+0.00	[+1.49]
cc-pV5Z	+2.26	−0.80	+0.05	+0.00	[+1.51]
CBS limit	[+2.27]	[−0.81]	[+0.05]	[+0.00]	**[+1.52]**
ΔE_v (final) = ΔE_e[CBS CCSD(T)] + Δ_{core}[CCSD(T)/cc-pCVTZ] + Δ_{ZPVE}[CCSD(T)/cc-pCVTZ] + Δ_{rel}[CCSD(T)/cc-pCVTZ] = +1.52 − 0.01 − 0.78 + 0.01 = **+0.74 kcal mol^{-1}**					
fit function	$a + be^{-cX}$	$a + bX^{-3}$	$a + bX^{-3}$	$a + bX^{-3}$	
points (X)	3, 4, 5	4, 5	4, 5	4, 5	

[a]The symbol δ denotes the increment in the relative energy (ΔE_e) with respect to the preceding level of theory in the hierarchy ROHF → MP2 → CCSD → CCSD(T). Square brackets signify results obtained from basis set extrapolations or additivity assumptions. Final predictions are boldfaced.

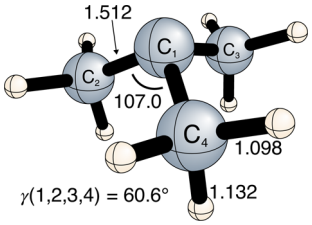

Figure 5. Structure of the ground state of the *t*-butyl anion (C_{3v} symmetry) optimized at the CCSD(T)/cc-pCVTZ level of theory. Bond lengths are in Ångstroms; angles are in degrees. The parameter γ(1,2,3,4) denotes the angle of the C_1−C_2 bond out of the C_1−C_3−C_4 plane. Only unique structural parameters are shown.

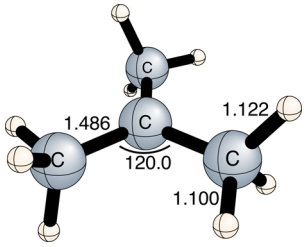

Figure 6. Structure of the C_{3h} transition state of the *t*-butyl anion optimized at the CCSD(T)/cc-pCVTZ level of theory. Bond lengths are in Ångstroms; angles are in degrees. Only unique structural parameters are shown.

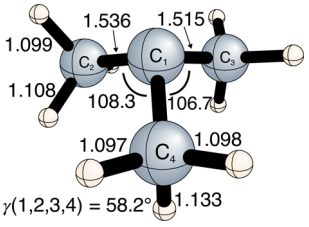

Figure 7. Structure of the C_s transition state of the *t*-butyl anion optimized at the CCSD(T)/cc-pCVTZ level of theory. Bond lengths are in Ångstroms; angles are in degrees. The parameter γ(1,2,3,4) denotes the angle of the C_1−C_2 bond out of the C_1−C_3−C_4 plane. Only unique structural parameters are shown.

Electron Affinity. The focal point analysis for the *t*-butyl radical adiabatic electron affinity (AEA) is shown in Table 2. The electron affinity computed at the Hartree−Fock (HF) level of theory extrapolated to the complete basis set (CBS) limit is −39.59 kcal mol^{-1}, suggesting that the formation of the anion is energetically unfavorable. The importance of electron correlation is already seen at the MP2/CBS level, which drastically corrects the HF result by a value of δ[MP2] = +41.57 kcal mol^{-1}, giving a qualitatively different prediction that favors the viability of the anion (Table 2). The successive addition of the corrections for full single, double, and perturbative triple excitations (δ[CCSD] = −8.92, δ[CCSD(T)] = +4.79 kcal mol^{-1}) proves that a rigorous treatment of electron correlation is absolutely essential to obtain the value of the AEA with an accuracy of 5 kcal mol^{-1}. Increments for full triples and perturbative quadruples are still significant (δ[CCSDT] = −0.20, δ[CCSDT(Q)] = +0.46 kcal mol^{-1}) but have much smaller values and nearly cancel each other, showing oscillatory convergence toward the full configuration interaction limit. The dependence of the predicted AEA value on the atomic-orbital basis set is also rather significant. The use of the aug-cc-pVXZ basis sets that include atomic orbitals of high angular momentum (X = Q, 5) augmented by diffuse functions is important, as illustrated by the difference of the δ[MP2] corrections at the MP2/aug-cc-pVDZ and MP2/CBS levels of theory. The strong method dependence of the AEA is in stark contrast to the aforementioned isomerization barriers, which are computed as the difference of two electronically similar structures; the electron affinity is computed as the difference of two structures with a different number of correlated electron pairs, which increases the sensitivity to the method used.

Combining the high-level treatment of electron correlation with extrapolation to the CBS limit yields a vibrationless AEA value of −1.88 kcal mol^{-1} for the *t*-butyl radical, at the CCSDT(Q)/CBS level of theory. The effect of zero-point vibrational energy on the AEA is taken into account by adding the auxiliary Δ_{ZPVE} = +2.01 and $\Delta_{aug-ZPVE}$ = −0.33 kcal mol^{-1} corrections. The correction for core correlation is much smaller (Δ_{core} = −0.29 kcal mol^{-1}) but is still important. The relativistic correction is almost negligible (Δ_{rel} = +0.01 kcal mol^{-1}). By adding all of the corrections described above to our CCSDT(Q)/CBS result, we obtain a *t*-butyl radical adiabatic electron affinity of −0.48 kcal mol^{-1}. The negative sign of the AEA indicates that the adiabatic formation of the anion is *t*-butyl energetically unfavorable. Given the oscillatory convergence toward the full CI limit, which is conducive to error cancellation, we can tentatively assign an error bar of ±0.5 kcal mol^{-1} to our result. Therefore, essentially all values spanned by the uncertainty in our final value are negative. Our predicted AEA value of −0.48 kcal mol^{-1} is in qualitative agreement with the majority of earlier experimental and theoretical results ranging from −3.2 to −9.5 kcal mol^{-1}, but with a much smaller absolute value.

Table 2. Focal Point Analysis of the Adiabatic Electron Affinity of the *t*-Butyl Radical (EA = *E*(radical) − *E*(anion), in kcal mol^{-1})[a]

basis set	EA[ROHF]	δ[MP2]	δ[CCSD]	δ[CCSD(T)]	δ[CCSDT]	δ[CCSDT(Q)]	EA[CCSDT(Q)]
aug-cc-pVDZ	−38.79	+38.28	−7.05	+4.13	−0.20	+0.46	[−3.17]
aug-cc-pVTZ	−39.58	+40.50	−8.48	+4.68	[−0.20]	[+0.46]	[−2.61]
aug-cc-pVQZ	−39.59	+41.01	−8.92	+4.79	[−0.20]	[+0.46]	[−2.44]
aug-cc-pV5Z	−39.59	+41.28	[−8.92]	[+4.79]	[−0.20]	[+0.46]	[−2.17]
CBS limit	[−39.59]	[+41.57]	[−8.92]	[+4.79]	[−0.20]	[+0.46]	[**−1.88**]
EA (final) = EA[CBS CCSDT(Q)] + Δ_{core}[CCSD(T)/aug-cc-pCVTZ] + Δ_{ZPVE}[CCSD(T)/cc-pCVTZ] + $\Delta_{aug-ZPVE}$[MP2/aug-cc-pVTZ] + Δ_{rel}[CCSD(T)/cc-pCVTZ] = −1.88 − 0.29 + 2.01 − 0.33 + 0.01 = **−0.48 kcal mol^{-1}**							
fit function	$a + be^{-cX}$	$a + bX^{-3}$	additive	additive	additive	additive	
points (X)	3,4,5	4,5					

[a]The symbol δ denotes the increment in the electron affinity (EA) with respect to the preceding level of theory in the hierarchy ROHF→MP2→CCSD→CCSD(T)→CCSDT→CCSDT(Q). Square brackets signify results obtained from basis set extrapolations or additivity assumptions. Final predictions are boldfaced.

Given the large degree of puckering observed upon attachment of an electron (*c.f.* Figures 1 and 5), we can expect a significant discrepancy between the adiabatic and the vertical electron affinities, i.e., those computed with and without geometry relaxation, respectively. At the CCSD(T)/aug-cc-pVTZ level of theory, the classical vertical electron affinity (VEA) is −10.5 kcal mol^{-1}, which is much larger than the corresponding adiabatic value of −2.9 kcal mol^{-1}. A more interesting corollary of the large geometric distortion is the seemingly metastable nature of the anion. Despite lying higher in energy than the radical, the vibrationless vertical detachment energy (VDE) of the anion is 10.6 kcal mol^{-1}, at the CCSD(T)/aug-cc-pVTZ level of theory, indicating that the *t*-butyl anion is classically metastable.

Inclusion of quantum mechanical zero-point vibrational energy effects (73.3 and 71.3 kcal mol^{-1} for the radical and anion, respectively, from the aforementioned harmonic vibrational analysis) corrects the classical picture and increases the ground state energy to a value far above the crossing point of the anion and neutral surfaces, as depicted in Figure 8. Applying the standard rigid rotor/harmonic oscillator treatment to obtain thermal corrections, we find that the thermal contribution to the Gibbs free energy at 298 K further raises the energy of the anion by 0.6 kcal mol^{-1}, relative to the neutral. Since the umbrella mode connecting the neutral and anion equilibrium structures is floppy, quantum mechanical effects do not favor the metastability of the *t*-butyl anion. Even if the *t*-butyl anion is unobservable by conventional photodetachment methods,[47] it might yet be detected by suitable electron scattering experiments.[48]

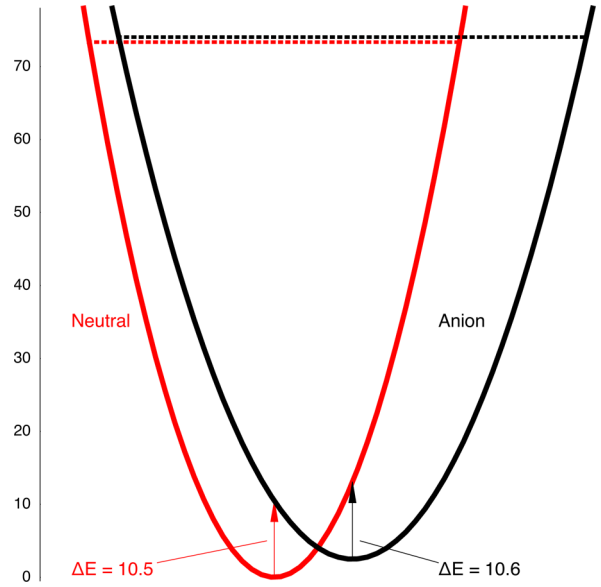

Figure 8. Schematic overview of the CCSD(T)/aug-cc-pVTZ relative energies (kcal mol^{-1}) of the *t*-butyl radical and its anion. The red and black arrows represent vibrationless vertical attachment and vertical detachment energies, respectively. The zero-point vibrational energy levels, from the vibrational frequencies described in the text, are depicted by dashed lines.

CONCLUSIONS

We have performed a theoretical study of the structures, harmonic vibrational frequencies, and electron affinity of the *t*-butyl radical using reliable coupled cluster methods. Three stationary points of C_{3v}, C_{3h}, and C_s symmetry were found on the ground state potential energy surface of the *t*-butyl radical. The global minimum structure has C_{3v} symmetry with a nonplanar carbon backbone. Comparison of the distances for the axial and equatorial C−H bonds of the methyl groups provides evidence for negative hyperconjugation interactions between the unpaired electron localized on the central carbon atom and the antibonding orbitals of the axial C−H bonds; natural orbital analysis confirms this finding. Negative hyperconjugation also manifests itself in longer C−H distances and lower C−H stretching frequencies for the axial C−H bonds. Transition states with C_{3h} and C_s symmetry, for pyramidal inversion and internal rotation of the methyl group, were also found. Their structures lie 0.73 and 0.85 kcal mol^{-1}, respectively, above the global minimum at the CCSD(T)/CBS level of theory and were also analyzed. For the *t*-butyl anion, we have also studied three structures of C_{3v}, C_{3h}, and C_s symmetry. These structures resemble those of the radical, but with much more puckered carbon backbones and larger isomerization barriers.

Using the convergent focal point analysis technique, we have computed the adiabatic electron affinity (AEA) of the *t*-butyl radical. The electron attachment is energetically unfavorable with a value of −0.48 kcal mol^{-1} at the CCSDT(Q)/CBS level of theory. Computations at the MP2 level of theory give qualitatively incorrect results, overestimating the value of the electron affinity and favoring the thermodynamic stability of the anion. The use of correlation treatments incorporating up to perturbative quadruple excitations, together with large augmented basis sets and zero-point vibrational corrections, is

important. When zero-point vibrational effects are not taken into account, the anion is found to be metastable.

The small magnitude of the *t*-butyl radical's gas-phase electron affinity indicates the possibility of designing derivatives that will bind an electron. In particular, the use of electron-withdrawing substituents, such as −F, $-CF_3$ or −CN, is expected to stabilize the anion.

■ ASSOCIATED CONTENT

Supporting Information

Tables S1−S5 showing harmonic vibrational frequencies of *t*-butyl radical and anion, results of the focal point analysis of the C_s *t*-butyl radical, and C_s and C_{3h} *t*-butyl anion energies. This material is available free of charge via the Internet at http://pubs.acs.org/.

■ AUTHOR INFORMATION

Corresponding Author

*E-mail: alex@ccqc.uga.edu.

Notes

The authors declare no competing financial interest.

■ ACKNOWLEDGMENTS

This research was supported by the U.S. Department of Energy, Office of Basic Energy Sciences, Combustion Program (Grant No. DEFG02-97-ER14748) and used resources of the National Energy Research Scientific Computing Center (NERSC), which is supported by the Office of Science of the U.S. Department of Energy under contract no. DE-AC02-05CH11231. We thank Professor Michael A. Duncan for insightful comments.

■ REFERENCES

(1) Mahaffy, P. R. *Science* **2005**, *308*, 969−970.
(2) Waite, J. H.; et al. *Science* **2005**, *308*, 982−986.
(3) Geem, K. M. V.; Dhuyvetter, I.; Prokopiev, S.; Reyniers, M.-F.; Viennet, D.; Marin, G. B. *Ind. Eng. Chem. Res.* **2009**, *48*, 10343−10358.
(4) Wauters, S.; Marin, G. B. *Ind. Eng. Chem. Res.* **2002**, *41*, 2379−2391.
(5) Clymans, P. J.; Froment, G. F. *Comput. Chem. Eng.* **1984**, *8*, 137−142.
(6) Geem, K. M. V.; Pyl, S. P.; Marin, G. B.; Harper, M. R.; Green, W. H. *Ind. Eng. Chem. Res.* **2010**, *49*, 10399−10420.
(7) Karwat, D. M.; Wagnon, S. W.; Teini, P. D.; Wooldridge, M. S. *J. Phys. Chem.* **2011**, *115*, 4909−4921.
(8) Harper, H. R.; Geem, K. M. V.; Pyl, S. P.; Marin, G. B.; Green, W. H. *Combust. Flame* **2011**, *158*, 16−41.
(9) Kochi, J. K. *Advances in Free Radical Chemistry*; Academic: New York, 1975; Vol. *5*.
(10) Wood, D. E.; Williams, L. F.; Sprecher, R. F.; Lathan, W. A. *J. Am. Chem. Soc.* **1972**, *94*, 6241−6243.
(11) Koenig, T.; Balle, T.; Snell, W. *J. Am. Chem. Soc.* **1975**, *97*, 662−663.
(12) Krusic, P. J.; Meakin, P. *J. Am. Chem. Soc.* **1976**, *98*, 228−230.
(13) Yoshimine, M.; Pacansky, J. *J. Chem. Phys.* **1981**, *74*, 5168−5173.
(14) Pacansky, J.; Chang, J. S. *J. Chem. Phys.* **1981**, *74*, 5539−5546.
(15) Paddon-Row, M. N.; Houk, K. N. *J. Am. Chem. Soc.* **1981**, *103*, 5046−5049.
(16) Pacansky, J.; Koch, W.; Miller, M. D. *J. Am. Chem. Soc.* **1991**, *113*, 317−328.
(17) Ignaczak, A. *J. Theor. Comput. Chem.* **2011**, *10*, 325−348.
(18) Schleyer, P. v. R.; Spitznagel, G. W. *Tetrahedron Lett.* **1986**, *27*, 4411−4414.
(19) DePuy, C. H.; Gronert, S.; Barlow, S. E.; Bierbaum, V. M.; Damrauer, R. *J. Am. Chem. Soc.* **1989**, *111*, 1968−1973.
(20) Vera, D. M. A.; Pierini, A. B. *Phys. Chem. Chem. Phys.* **2004**, *6*, 2899−2903.
(21) Sauers, R. R. *Tetrahedron* **1999**, *55*, 10013−10026.
(22) Petrou, P. S.; Nicolaides, A. V. *Tetrahedron* **2008**, *65*, 1655−1659.
(23) Feng, H.; Sun, W.; Xie, Y.; Schaefer, H. F. *Chem.—Eur. J.* **2011**, *17*, 10552−10555.
(24) Rittby, M.; Bartlett, R. J. *J. Phys. Chem.* **1988**, *92*, 3033−3036.
(25) Stanton, J. F.; Gauss, J.; Watts, J. D.; Bartlett, R. J. *J. Chem. Phys.* **1991**, *94*, 4334−4345.
(26) Hampel, C.; Peterson, K. A.; Werner, H.-J. *Chem. Phys. Lett.* **1992**, *190*, 1−12.
(27) Watts, J. D.; Gauss, J.; Bartlett, R. J. *Chem. Phys. Lett.* **1992**, *200*, 1−7.
(28) Raghavachari, K.; Trucks, G. W.; Pople, J. A.; Head-Gordon, M. *Chem. Phys. Lett.* **1989**, *157*, 479−483.
(29) Stanton, J. F. *Chem. Phys. Lett.* **1997**, *281*, 130−134.
(30) Dunning, T. H. *J. Chem. Phys.* **1989**, *90*, 1007−1023.
(31) Woon, D. E.; Dunning, T. H. *J. Chem. Phys.* **1995**, *103*, 4572−4585.
(32) East, A. L. L.; Allen, W. D. *J. Chem. Phys.* **1993**, *99*, 4638−4650.
(33) Simmonett, A. C.; Schaefer, H. F.; Allen, W. D. *J. Chem. Phys.* **2009**, *130*, 044301−044301−10.
(34) Feller, D. *J. Chem. Phys.* **1993**, *98*, 7059−7071.
(35) Helgaker, T.; Klopper, W.; Koch, H.; Noga, J. *J. Chem. Phys.* **1997**, *106*, 9639−9646.
(36) Bomble, Y. J.; Stanton, J. F.; Kállay, M.; Gauss, J. *J. Chem. Phys.* **2005**, *123*, 054101−054101−8.
(37) Stanton, J. F.; Gauss, J.; Watts, J. D.; Szalay, P. G.; Bartlett, R. J.; Auer, A. A.; Bernholdt, D. E.; Christiansen, O.; Harding, M. E.; Heckert, M.; Heun, O.; Huber, C.; Jonsson, D.; Jusélius, J.; Lauderdale, W. J.; Metzroth, T.; Michauk, C.; O'Neill, D. P.; Price, D. R.; Ruud, K.; Schiffmann, F.; Tajti, A.; Varner, M. E.; Vázquez, J. *CFOUR*; integral packages *Molecule* (Almlöf, J.; Taylor, P. R.), *Props* (Taylor, P. R.), and *Abacus* (Helgaker, T.; Jensen, H. J. Aa.; Jørgensen, P.; Olsen, J.); and ECP routines (Mitin, A. V. van Wüllen, C.). For the current version see, http://www.cfour.de (accessed October 2012).
(38) Werner, H. J.; Knowles, P. J.; Knizia, G.; Manby, F. R.; Schütz, M.; Celani, P.; Korona, T.; Lindh, R.; Mitrushenkov, A.; Rauhut, G.; Shamasundar, K. R.; Adler, T. B.; Amos, R. D.; Bernhardsson, A.; Berning, A.; Cooper, D. L.; Deegan, M. J. O.; Dobbyn, A. J.; Eckert, F.; Goll, E.; Hampel, C.; Hesselmann, A.; Hetzer, G.; Hrenar, T.; Jansen, G.; Köppl, C.; Liu, Y.; Lloyd, A. W.; Mata, R. A.; May, A. J.; McNicholas, S. J.; Meyer, W.; Mura, M. E.; Nicklass, A.; O'Neill, D. P.; Palmieri, P.; Pflüger, K.; Pitzer, R.; Reiher, M.; Shiozaki, T.; Stoll, H.; Stone, A. J.; Tarroni, R.; Thorsteinsson, T.; Wang, M.; Wolf, A. *MOLPRO*, version 2010.1; Cardiff University: Cardiff, U. K.; Universität Stuttgart: Stuttgart, Germany, 2010. See http://www.molpro.net (accessed October 2012).
(39) Kállay, M.; Surján, P. *J. Chem. Phys.* **2001**, *115*, 2945−2954.
(40) Kállay, M.; Gauss, J. *J. Chem. Phys.* **2005**, *123*, 214105−214105−13.
(41) Alabugin, I. V.; Gilmore, K. M.; Peterson, P. W. *WIREs Comput. Mol. Sci.* **2011**, *1*, 109−141.
(42) Weinhold, F. *Nature* **2001**, *411*, 539−541.
(43) Hoffmann, R.; Radom, L.; Pople, J. A.; Schleyer, P. v. R.; Hehre, W. J.; Salem, L. *J. Am. Chem. Soc.* **1972**, *94*, 6221−6223.
(44) Jarowski, P. D.; Wodrich, M. D.; Wannere, C. S.; Schleyer, P. v. R.; Houk, K. N. *J. Am. Chem. Soc.* **2004**, *126*, 15036−15037.
(45) Reed, A. E.; Weinstock, R. B.; Weinhold, F. *J. Chem. Phys.* **1985**, *83*, 735−746.
(46) Reed, A. E.; Curtiss, L. A.; Weinhold, F. *Chem. Rev.* **1988**, *88*, 899−926.
(47) Wren, S. W.; Vogelhuber, K. M.; Ervin, K. M.; Lineberger, W. C. *Phys. Chem. Chem. Phys.* **2009**, *11*, 4745−4753.

(48) Robertson, W. D.; Hammer, N. I.; Bartmess, J. E.; Compton, R. N.; Diri, K.; Jordan, K. D. *J. Chem. Phys.* **2005**, *122*, 204319−204319−6.